JJAP Japanese Journal of Applied Physics ISSN Online:1347-4065 / Print:0021-4922

Jpn. J. Appl. Phys. **52** (2013) 060204 (4 pages) |Previous Article| |Next Article| |Table of Contents|
|Full Text PDF (632K)| |Buy This Article|

Rapid Communication

High-Performance Amorphous Indium Oxide Thin-Film Transistors Fabricated by an Aqueous Solution Process at Low Temperature

Kookhyun Choi, Minseok Kim, Seongpil Chang, Tae-Yeon Oh, Shin Woo Jeong, Hyeon Jun Ha, and Byeong-Kwon Ju

Display and Nanosystem Laboratory, Department of Electrical Engineering, Korea University, Seoul 136-713, Republic of Korea

(Received February 28, 2013; accepted May 8, 2013; published online May 31, 2013)

This paper presents low temperature solution-processed fabrication techniques for modern thin-film transistors (TFTs). We have investigated the electrical performance of aqueous solution-processed amorphous indium oxide (a-In_2O_3) TFTs prepared using different annealing temperatures. Even though the a-In_2O_3 TFTs were annealed at 200 °C, electrical characteristics of aqueous solution-processed a-In_2O_3 TFTs were obtained. High performance such as a saturation mobility of 8.6 $cm^2 V^{-1} s^{-1}$ and an on/off current ratio of over 10^6 was exhibited by a-In_2O_3 TFTs annealed at 250 °C.

URL: http://jjap.jsap.jp/link?JJAP/52/060204/
DOI: 10.7567/JJAP.52.060204

|Full Text PDF (632K)| |Buy This Article| Citation: Plain Text view

References

1. D. Guo, S. Ikeda, K. Saiki, H. Miyazoe, and K. Terashima: J. Appl. Phys. **99** (2006) 094502[AIP Scitation].
2. H. Y. Choi, S. H. Kim, and J. Jang: Adv. Mater. **16** (2004) 732[CrossRef].
3. C.-S. Yang, L. L. Smith, C. B. Arthur, and G. N. Parsons: J. Vac. Sci. Technol. B **18** (2000) 683[AIP Scitation].
4. P. G. Carey, P. M. Smith, S. D. Theiss, and P. Wickboldt: J. Vac. Sci. Technol. A **17** (1999) 1946[AIP Scitation].
5. A. Sazonov and A. Nathan: J. Vac. Sci. Technol. A **18** (2000) 780[AIP Scitation].
6. K. Nomura, H. Ohta, A. Takagi, T. Kamiya, M. Hirano, and H. Hosono: Nature **432** (2004) 488[CrossRef].
7. P. F. Carcia, R. S. McLean, M. H. Reilly, and G. Nunes, Jr.: Appl. Phys. Lett. **82** (2003) 1117[AIP Scitation].
8. S.-Y. Han, G. S. Herman, and C.-H. Chang: J. Am. Chem. Soc. **133** (2011) 5166[CrossRef].
9. B. Yaglioglu, H. Y. Yeom, R. Beresford, and D. C. Paine: Appl. Phys. Lett. **89** (2006) 062103[AIP Scitation].
10. J.-H. Jeon, Y. H. Hwang, J. Jin, and B.-S. Bae: MRS Commun. **2** (2012) 17.
11. K.-H. Choi, H.-J. Nam, J.-A. Jeong, S.-W. Cho, H.-K. Kim, J.-W. Kang, D.-G. Kim, and W.-J. Cho: Appl. Phys. Lett. **92** (2008) 223302[AIP Scitation].
12. A. Suresh, P. Wellenius, A. Dhawan, and J. Muth: Appl. Phys. Lett. **90** (2007) 123512[AIP Scitation].
13. S. Masuda, K. Kitamura, Y. Okumura, S. Miyatake, H. Tabata, and T. Kawai: J. Appl. Phys. **93** (2003) 1624[AIP Scitation].
14. S.-J. Seo, C. G. Choi, Y. H. Hwang, and B.-S. Bae: J. Phys. D **42** (2009) 035106[IoP STACKS].

High-Performance Amorphous Indium Oxide Thin-Film Transistors Fabricated by an Aqueous Solution Process at Low Temperature

2013 Jpn. J. Appl. Phys. 52 060204

(http://iopscience.iop.org/1347-4065/52/6R/060204)

Japanese Journal of Applied Physics **52** (2013) 060204 **RAPID COMMUNICATION**
http://dx.doi.org/**10.7567/JJAP.52.060204**

High-Performance Amorphous Indium Oxide Thin-Film Transistors Fabricated by an Aqueous Solution Process at Low Temperature

Kookhyun Choi, Minseok Kim, Seongpil Chang, Tae-Yeon Oh, Shin Woo Jeong, Hyeon Jun Ha, and Byeong-Kwon Ju*

Display and Nanosystem Laboratory, Department of Electrical Engineering, Korea University, Seoul 136-713, Republic of Korea
E-mail: bkju@korea.ac.kr

Received February 28, 2013; accepted May 8, 2013; published online May 31, 2013

This paper presents low temperature solution-processed fabrication techniques for modern thin-film transistors (TFTs). We have investigated the electrical performance of aqueous solution-processed amorphous indium oxide (a-In_2O_3) TFTs prepared using different annealing temperatures. Even though the a-In_2O_3 TFTs were annealed at 200 °C, electrical characteristics of aqueous solution-processed a-In_2O_3 TFTs were obtained. High performance such as a saturation mobility of 8.6 $cm^2 V^{-1} s^{-1}$ and an on/off current ratio of over 10^6 was exhibited by a-In_2O_3 TFTs annealed at 250 °C. © 2013 The Japan Society of Applied Physics

The limitation of thin-film transistors (TFTs) based on conventional amorphous silicon (a-Si) has become a challenging issue for switching devices in recent years. Organic semiconductors [e.g., pentacene, poly(3-hexylthiophene)], hydrogenated a-Si (a-Si:H), and oxide semiconductors have been investigated for use as new semiconducting materials in advanced displays.[1–5] However, these materials are not sufficient for high-performance displays (e.g., active-matrix organic light-emitting diodes) in terms of electrical properties. On the other hand, oxide semiconductors have many advantages such as high transparency in the visible region (400–700 nm), wide band gap ($E_g > 3.1$ eV), good uniformity, and high mobility.[6] Many published papers have reported research on binary oxides (ZnO, In_2O_3), ternary oxides (In–Zn–O, Zn–Sn–O), and quaternary oxides (In–Zn–Sn–O, In–Ga–Zn–O) and the production of oxide-semiconductor-based TFTs.[7–12] Indium oxide (In_2O_3) has been commonly used because it can provide the high mobility originating from the *ns* orbital of the metal cation that is larger than the 2p orbital of oxygen anion. Indium-oxide-based semiconductors thus have promises of high performance. Indium oxide is also one of the oxide-based semiconducting materials that can be applied to the solution process and exhibit various electrical characteristics such as conductivity and semiconductivity depending on the stoichiometry and defects in the material.[8] Among oxide semiconductors, amorphous oxide semiconductors exhibit better surface uniformity than polycrystalline oxide semiconductors (e.g., ZnO).[13] Recently, the solution process has received much attention owing to the simplicity of its use in the deposition of oxide semiconductors as well as the possibility to apply the technique to large-scale displays. Until now, many researchers have synthesized the solution using an alcohol-based solvent for oxide semiconductors. Although the process has required a high annealing temperature of up to 400 °C,[14–16] it is essential to lower the process temperature for applications in TFT fabrication on flexible substrates. In recent years, there have been reports on the combustion process involving metal oxide semiconductors. To complicate matters, it has been reported that indium chloride and ethyleneglycol are used as the metal precursor and reagent, respectively, to enhance the formation of thin films.[8,17] Although solution-based oxide TFTs with high performances have been demonstrated at low temperatures (less than 300 °C), harmful solvents such as 2-methoxyethanol and acetonitrile are still used in the synthesis process. Therefore, in this paper, an aqueous solution process using de-ionized water (DI water) is employed as a safe and harmless solvent. In our aqueous solution process, only DI water (in place of alcohol-based solvents) is used to dissolve the metal precursor. Moreover, the process does not need any chemical materials for stabilization in our study. The aqueous solution process is not only low-temperature, harmless, and cost-effective, it is very simple. Here, we suggest possibilities of applying the technique on flexible substrates in a low-temperature process, focusing on the fabrication of high-performance devices using an alcohol-free and low-cost solvent.

To produce the metal-precursor, indium(III) nitrate hydrate [$In(NO_3)_3 \cdot xH_2O$; Sigma Aldrich] was dissolved in DI water. A prepared solution of 0.2 M In_2O_3 was stirred for 3 h at 80 °C and then exposed to be homogenized in air for over 24 h.[18] Heavily doped p^{++} Si wafers ($\rho < 0.01\ \Omega$ cm) were used as substrates. A thermally oxidized 300-nm SiO_2 layer deposited on the Si wafer was used as the gate insulator. The substrates were cleaned successively using acetone, methanol, and isopropyl-alcohol in an ultrasonic bath for 15 min at 45 °C. After the cleaning processes, surface treatment in an oxygen plasma system (Femto Science CUTE-MP/R) was performed for 5 min to provide a hydrophilic surface on each substrate. The In_2O_3 solution was released through a 0.2-μm poly(tetrafluoroethylene) filter and spin-coated at 3,000 rpm for 35 s. The substrates were then annealed on a hotplate at 200–400 °C under ambient air. The thermal behavior of the sol–gel precursors was monitored under an air atmosphere using a thermal-gravimetric analyzer (TGA; Setaram Setsys 16/18) with a scanning rate of 10 °C/min. The amorphous structure and surface morphology of a-In_2O_3 thin films were measured with an X-ray diffractometer (XRD; Rigaku MAX-2500V) and an atomic force microscope (AFM; Park Systems XE-100), respectively. The microstructure of the a-In_2O_3 thin films was investigated using a field emission transmission electron microscope (FE-TEM; FEI Tecnai G2 F30). In the a-In_2O_3 TFT fabrication, a 100-nm aluminum (Al) layer was deposited by thermal evaporation through a metal shadow mask to form the top-contact source and drain electrodes. The channel length (L) and width (W) were 70 and 3000 μm, respectively. The electrical characteristics of a-In_2O_3 TFTs were confirmed using a semiconductor characterization system (Keithley 4200-SCS) in a dark box.

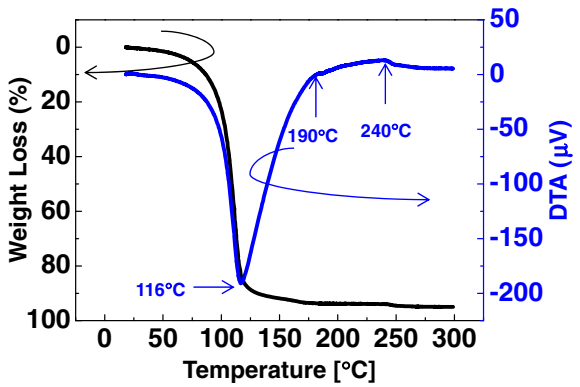

Fig. 1. (Color online) TGA of the 0.2 M In_2O_3 precursor solution.

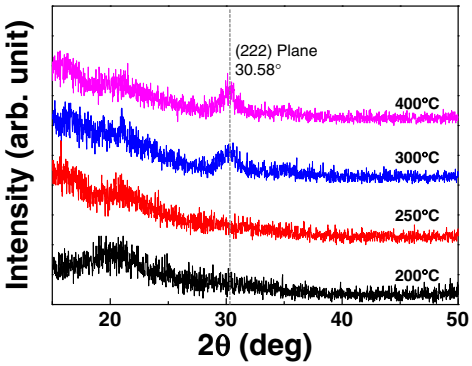

Fig. 2. (Color online) XRD spectra of a-In_2O_3 thin films spin-coated on SiO_2–Si substrates.

Transmittance of the a-In_2O_3 thin films was investigated using an UV-vis-NIR spectrophotometer (Agilent Carry 5000).

To determine the heat-treatment temperature, TGA was performed under ambient air. Figure 1 shows the thermal behavior of the In_2O_3 precursor solution. The dominant weight loss with an endothermic peak that occurred at 116 °C was a result of evaporation of water, which was used as the aqueous solution without organic solvents and additives. Above 116 °C, two steps of weight loss were observed, with the first step indicating thermal decomposition of metal nitrate at 190 °C. The second step represented the evaporation of volatile nitrate precursor at 240 °C, as shown by in the following chemical reaction:

$$In(NO_3)_3 \cdot xH_2O + H_2O \rightarrow HO\text{–}In\text{–}O\text{–}In\text{–}N + H_2O. \quad (1)$$

No noticeable heat transfer was observed above 240 °C. This exothermic reaction was attributed to the dehydroxylation of M–OH and polycondensation ($MO + xH_2O\uparrow$).[19,20] Thermal analysis of the In_2O_3 solution indicated that the semiconducting characteristics would be distinguishable after annealing at a temperature above 240 °C. The M–O–M network originated from a nucleophilic reaction between different metal monomeric species in the aqueous solution. Conventional methods usually form M–O–M networks during annealing through the interaction between a coated liquid film and water molecules in ambient air. In this study, hydrolysis and condensation of the aqueous solution already formed M–O–M networks that lowered the kinetic energy required to form oxide material during annealing, resulting in a low processing temperature of 240 °C, as shown in Fig. 1.[21]

To define the microstructure of the In_2O_3 films, XRD was carried out for films with different annealing temperatures, as shown in Fig. 2. The diffraction profiles suggested that the films had an amorphous structure because no sharp peaks were observed after the annealing processes at both 200 and 250 °C. For the annealing temperatures of both 300 and 400 °C, a sharper peak at $2\theta = 30.58°$ that corresponded to the (222) orientation of polycrystalline In_2O_3 was observed. In general, In_2O_3 thin films have been reported to exhibit the bixbyite-type cubic structure.[22,23] On the other hand, in the case of thin metal oxide layers (less than 20 nm thick), the amorphous structure can remain up to a temperature of

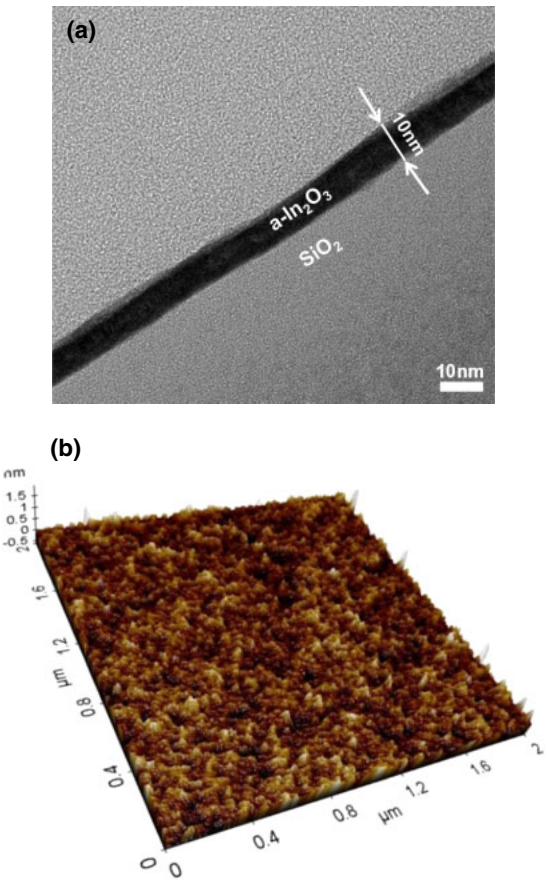

Fig. 3. (Color online) (a) FE-TEM image of the In_2O_3 cross-sectional structure. (b) AFM image of the a-In_2O_3 thin film. The rms roughness was about 0.2 nm. The devices were annealed at 250 °C.

~250 °C owing to their structural disorder.[24,25] Our research results agreed with these reports. Therefore, the sample cured at 250 °C was optimized for In_2O_3 TFT fabrication in our study.

Figure 3(a) shows the cross-sectional TEM image of an In_2O_3 thin film with a thickness of 10 nm, which confirms the amorphous structure of the In_2O_3 thin film annealed at 250 °C. The film thickness of 10 nm was optimized for the channel layer in an a-In_2O_3 TFT in order to avoid excessive background carrier effects by reducing the carrier transport

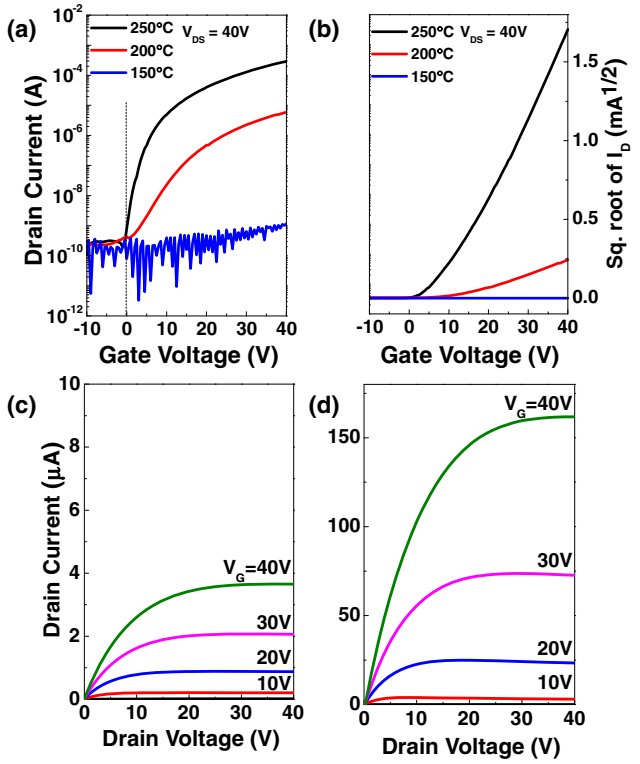

Fig. 4. (Color online) (a) Transfer characteristics of a-In_2O_3 TFTs depending on annealing temperature. (b) Plot of $(I_D)^{1/2}$ versus V_G depending on annealing temperature. Output characteristics of a-In_2O_3 TFTs annealed at (c) 200 °C and (d) 250 °C.

Table I. Summary of electrical characteristics of a-In_2O_3 TFTs prepared using different annealing temperatures. $In(NO_3)_3 \cdot xH_2O$ concentration is 0.2 M.

Annealing temp. (°C)	μ_{sat} ($cm^2\,V^{-1}\,s^{-1}$)	$I_{on/off}$	V_T (V)	S (V/decade)
150	N/A	—	—	—
200	1.0	3.2×10^5	15.3	2.4
250	8.6	5.4×10^6	5.1	1.8

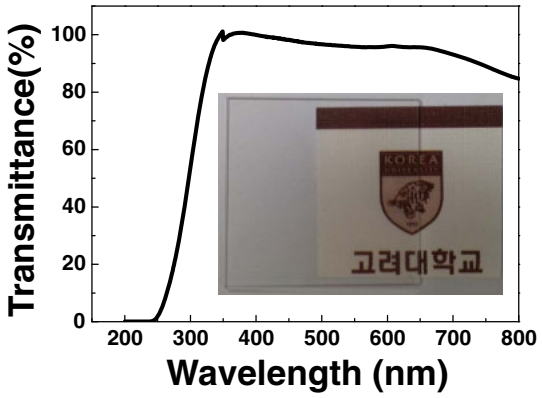

Fig. 5. (Color online) Transmittance of a-In_2O_3 TFTs annealed at 250 °C.

resulting from scattering in the interfacial channel region.[26] Figure 3(b) shows the smooth surface seen in an AFM morphological image of the a-In_2O_3 thin film with a root-mean-square (rms) surface roughness of about 0.2 nm. Note that the device performance was strongly dependent on the surface roughness of the sol–gel-processed In_2O_3 film in our study.

For the investigation of the electrical properties of a-In_2O_3 TFTs, the mobility of these TFTs was estimated using a linear fit of the $I_D^{1/2}$ versus V_G curve and applying Eq. (2) for a field-effect transistor in the saturation region ($V_D > V_G - V_T$):[27]

$$I_D = \left(\frac{C_i \mu_{sat} W}{2L}\right)(V_G - V_T)^2, \quad (2)$$

where I_D and V_D are the source-to-drain current and voltage, respectively; C_i is the capacitance per unit area of the gate insulator; V_G is the voltage of the gate; V_T is the threshold voltage. The value of V_T was extracted from the x-axis intercept of the line obtained by plotting the square root of I_D versus V_G. The subthreshold swing (S), which evaluates how rapidly the TFT switches between the off state and the on state in the region of exponential current increase, was estimated by the following equation:

$$S = \left(\frac{d|\log_{10} I_D|}{dV_G}\right)^{-1}. \quad (3)$$

When an annealing temperature of 150 °C was used, the device was not operational since the nitrate precursor and absorbed moisture were not decomposed and there was no evaporation. However, the thermal decomposition of metal nitrate occurred at 190 °C, as shown in Fig. 1. The transfer and output curves shown in Fig. 4 are the results of one-way measurement. It was confirmed that the TFT annealed at 200 °C exhibited a saturation mobility (μ_{sat}) of 1.0 $cm^2\,V^{-1}\,s^{-1}$, an on/off current ratio ($I_{on/off}$) of 3.2×10^5, V_T of 15.3 V, and S of 2.4 V/decade. In the case of In_2O_3 annealing at 250 °C, the highest performance was obtained with μ_{sat} of 8.6 $cm^2\,V^{-1}\,s^{-1}$, $I_{on/off}$ of 5.4×10^6, V_T of 5.1 V, and S of 1.8 V/decade. When the V_G was 6 V at V_D of 40 V, the hysteresis (ΔV_{th}) values was 3 V. In case of the In_2O_3 film annealed at 300 °C, the TFTs showed nonsaturated electrical properties because of the crystallized In_2O_3 structure shown in Fig. 2. The crystallized a-In_2O_3 thin films were too conductive to serve as semiconducting layers (the figure did not show). All the device characteristics are summarized in Table I. As can be seen in Fig. 5, an a-In_2O_3 thin film annealed on a glass substrate at 250 °C showed an optical transmittance of over 98% in the visible light region; the image beneath the sample was clearly visible.

We demonstrated the fabrication of high-performance a-In_2O_3 TFTs via an aqueous solution process that can be fabricated at low temperature because of its use of nonorganic solvents. The a-In_2O_3 TFTs annealed at 250 °C showed high performance with a saturation mobility of ~8.6 $cm^2\,V^{-1}\,s^{-1}$ and an on/off current ratio of greater than $\sim 10^6$. Even a-In_2O_3 TFTs annealed at 200 °C exhibited reasonable properties, with a saturation mobility of ~1.0 $cm^2\,V^{-1}\,s^{-1}$ and an on/off current ratio of $\sim 10^5$. We believe that this achievement allows us to apply solution-processable TFTs towards realization of the manufacture of flexible electronics.

Acknowledgements This work was partly supported by the IT R&D program of MKE/KEIT (Grant No. 10041416, The core technology development of light and space adaptable new mode display for energy saving on 7-in. and 2 W), the IT R&D Program of MOTIE/KEIT (KI002104, Development of Fundamental Technologies for Flexible Combined-Function Organic Electronic Device) and the MKE, Korea, under the IT R&D Infrastructure Program supervised by the NIPA (National IT Industry Promotion Agency) [NIPA-2011-(B1110-1101-0002)], and a Korea University Grant.

1) D. Guo, S. Ikeda, K. Saiki, H. Miyazoe, and K. Terashima: J. Appl. Phys. **99** (2006) 094502.
2) H. Y. Choi, S. H. Kim, and J. Jang: Adv. Mater. **16** (2004) 732.
3) C.-S. Yang, L. L. Smith, C. B. Arthur, and G. N. Parsons: J. Vac. Sci. Technol. B **18** (2000) 683.
4) P. G. Carey, P. M. Smith, S. D. Theiss, and P. Wickboldt: J. Vac. Sci. Technol. A **17** (1999) 1946.
5) A. Sazonov and A. Nathan: J. Vac. Sci. Technol. A **18** (2000) 780.
6) K. Nomura, H. Ohta, A. Takagi, T. Kamiya, M. Hirano, and H. Hosono: Nature **432** (2004) 488.
7) P. F. Carcia, R. S. McLean, M. H. Reilly, and G. Nunes, Jr.: Appl. Phys. Lett. **82** (2003) 1117.
8) S.-Y. Han, G. S. Herman, and C.-H. Chang: J. Am. Chem. Soc. **133** (2011) 5166.
9) B. Yaglioglu, H. Y. Yeom, R. Beresford, and D. C. Paine: Appl. Phys. Lett. **89** (2006) 062103.
10) J.-H. Jeon, Y. H. Hwang, J. Jin, and B.-S. Bae: MRS Commun. **2** (2012) 17.
11) K.-H. Choi, H.-J. Nam, J.-A. Jeong, S.-W. Cho, H.-K. Kim, J.-W. Kang, D.-G. Kim, and W.-J. Cho: Appl. Phys. Lett. **92** (2008) 223302.
12) A. Suresh, P. Wellenius, A. Dhawan, and J. Muth: Appl. Phys. Lett. **90** (2007) 123512.
13) S. Masuda, K. Kitamura, Y. Okumura, S. Miyatake, H. Tabata, and T. Kawai: J. Appl. Phys. **93** (2003) 1624.
14) S.-J. Seo, C. G. Choi, Y. H. Hwang, and B.-S. Bae: J. Phys. D **42** (2009) 035106.
15) B. S. Ong, C. Li, Y. Li, Y. Wu, and R. Loutfy: J. Am. Chem. Soc. **129** (2007) 2750.
16) C. Avis and J. Jang: J. Mater. Chem. **21** (2011) 10649.
17) M.-G. Kim, M. G. Kanatzidis, A. Facchetti, and T. J. Marks: Nat. Mater. **10** (2011) 382.
18) R. B. H. Tahar, T. Ban, Y. Ohya, and Y. Takahashi: J. Appl. Phys. **82** (1997) 865.
19) D. Kim, C. Y. Koo, K. Song, Y. Jeong, and J. Moon: Appl. Phys. Lett. **95** (2009) 103501.
20) S. Jeong, Y. Jeong, and J. Moon: J. Phys. Chem. C **112** (2008) 11082.
21) D. H. Lee, Y. J. Chang, G. S. Herman, and C. H. Chang: Adv. Mater. **19** (2007) 843.
22) O. M. Berengue, A. D. Rodrigues, C. J. Dalmaschio, A. J. C. Lanfredi, E. R. Leite, and A. J. Chiquito: J. Phys. D **43** (2010) 045401.
23) J. Rosen and O. Warschkow: Phys. Rev. B **80** (2009) 115215.
24) H. H. Hsieh and C. C. Wu: Appl. Phys. Lett. **91** (2007) 013502.
25) J.-S. Park, J. K. Jeong, H.-J. Chung, Y.-G. Mo, and H. D. Kim: Appl. Phys. Lett. **92** (2008) 072104.
26) J. H. Noh, S. Y. Ryu, S. J. Jo, C. S. Kim, S.-W. Sohn, P. D. Rack, D.-J. Kim, and H. K. Baik: IEEE Electron Device Lett. **31** (2010) 567.
27) S. Chang, K.-Y. Dong, J.-H. Park, T.-Y. Oh, J.-W. Kim, S. Y. Lee, and B.-K. Ju: Appl. Phys. Lett. **92** (2008) 192104.